Desalination and Water Treatment
www.deswater.com
doi: 10.1080/19443994.2014.903208

54 (2015) 2825–2831
May

Taylor & Francis
Taylor & Francis Group

Enhanced salt-adsorption capacity of ambient pressure dried carbon aerogel activated by CO_2 for capacitive deionization application

D.K. Kohli, R. Singh*, A. Singh, S. Bhartiya, M.K. Singh, P.K. Gupta

Nano Functional Materials Laboratory, Laser Materials Development and Devices Division, Raja Ramanna Centre for Advanced Technology, Indore 452013, India, Tel. +91 731 2442691, Fax: +91 731 2488650; email: rashmi@rrcat.gov.in

Received 25 October 2013; Accepted 5 March 2014

ABSTRACT

Carbon aerogels (CAs) were prepared by polycondensation of resorcinol and formaldehyde using ambient drying technique and were further activated by CO_2. These were investigated for capacitive deionization (CDI) application. The gel parameters were optimized to obtain mesoporous CA with pore size distribution in 8–10 nm. The CA was further subjected to CO_2 activation at 950°C for different time durations and its effect on surface properties was studied. The surface area of the activated CA increased from 698 to 2057 m^2/g with corresponding increase in mesopore area from 289 to 644 m^2/g. The pore volume also increased from 0.79 to 1.72 cm^3/g. Cyclic voltammetry was performed on the test electrodes and specific capacitance values of 108 F/g was measured at scan rate of 10 mV/s in 1 M NaCl. Electrodes of size 200 × 200 mm were synthesized with an active material loading of ~15 mg/cm^2 and their CDI performance was evaluated in batch mode experiment. Salt-adsorption capacity as high as 8.4 mg/g for CO_2 activated CA was achieved for the starting electrolyte concentration of 500 mg/L, whereas the adsorption capacity for the CA without activation was 4.1 mg/g. The results suggest that CO_2 activated CA is a good choice for CDI application.

Keywords: Carbon aerogel; CO_2 activation; Capacitive deionization; Ambient drying; Adsorption capacity

1. Introduction

Energy efficient desalination technologies are required to meet the growing scarcity of potable water owing to population increase and industrial development. Capacitive deionization (CDI) is a promising method for removing dissolved salts by electrostatic adsorption reaction. The technique is mainly applicable for brackish water and offers advantage of easy regeneration, low voltage, and ambient operational conditions. CDI process is emerging as an energy-efficient alternative to the established desalination technologies, such as ion exchange, reverse osmosis, electrodialysis, and evaporation. Apart from high-energy efficiency it offers the advantages of long life cycle and non-secondary pollution [1,2].

One of the key factors that has limited scaling up of CDI technology is the availability of electrode material that can be mass produced at low cost and has high salt-adsorption capacity. Significant efforts have been focused on the preparation of various electrode materials to obtain higher CDI performance. Accordingly, different high surface area conducting materials including activated carbon (AC) [3], carbon

*Corresponding author.

nanotubes (CNT) [4], graphene [5], ordered mesoporous carbon (OMC) [6], and carbon aerogel (CA) [7] and their composites [8,9] have been investigated as electrode material for CDI. Salt-adsorption capacity of electrode material depends on the available surface area and the pore size distribution (PSD) of material. Although for AC the surface area is very large compared to that for CA and CNT, the accessible surface area is low due to dominance of micropores. This offsets the advantage of large surface area and results in comparable salt-adsorption capacity for these materials. Reported values for salt adsorption are 3.68 for AC, 3.32 for CNT, and 3.33 mg/g for CA [10–12]. Even though OMC value of salt adsorption is high 10.56 mg/g [13], these are too expensive from a commercial point of view. Recent studies have been made on composite electrode to utilize the advantage of complimentary surface characteristics of high surface area and PSD for improving CDI performance [14,15].

CAs are of interest for CDI application as they have good electrical conductivities and their surface area properties can be tailored by optimizing preparation conditions. CAs are generally synthesized via poly-condensation of formaldehyde with a phenol derivative in aqueous medium followed by supercritical drying [16]. Supercritical drying is costly, time consuming, and requires high-pressure operation. This leads to an uncompetitive price to performance ratio and thus limits commercial viability for large-scale production of CA. Therefore, alternative methods of CA synthesis using ambient drying conditions have been explored to suit the requirement of large-scale production. However, these have limitations of moderate surface area due to suppressed porosity [17–19]. CO_2 activation at elevated temperatures has proven very effective for improving surface area by widening of narrow microporosity and creating new pores in carbon materials [20]. This high surface area can be fully accessible only if there is proper PSD which provides good balance between micro and mesopore. It is well known that catalyzing condition during gel preparation of CA controls the size of interconnected particles and pores in the gel [21]. These need to be optimized for producing CA with high surface area and appropriate PSD that would improve salt-adsorption capacity of CDI electrode.

The objective of the present work was to produce CA with desired porosity by low cost ambient drying method. Resorcinol to catalyst ratio during synthesis was optimized to obtain proper pore size along with high surface area. Textural properties of CA were improved by CO_2 activation. Effect of different CO_2 activation conditions on surface area, pore volume, and PSD was investigated. Electrochemical performance was studied by cyclic voltametry and performance of the electrodes prepared with optimized conditions was studied in a CDI test cell.

2. Experimental

2.1. Synthesis of CA

CAs were synthesized by polycondensation of resorcinol (R) and formaldehyde (F) in an aqueous solution in a manner similar to the method used by Lee [22]. RF solution was prepared in water with molar ratio of R/F fixed at 0.5 and weight percent of reactants at 40% in the solution. Sodium carbonate was added as base catalyzing agent (C) to the solution in varying concentration to have different R/C molar ratio. Samples were designated as RFC-100, RFC-200, RFC-300, RFC-400, and RFC-500 for R/C molar ratios of 100, 200, 300, 400, and 500, respectively. The RF solution was gelled for ~70 h in a convection oven at 80˚C. After complete gelation water from the gel was exchanged with acetone at regular intervals. The density of the solvent was measured after every exchange to ensure complete water removal. Ambient drying of gel was then done at room temperature for two days. Finally, the dried aerogels were pyrolysed at 850˚C in a tubular furnace under inert atmosphere. The pyrolysed sample was treated at 950˚C under controlled atmosphere of CO_2 for varying time durations. The CO_2 gas was purged in presence of argon gas with CO_2/Ar ratio of 3:1 at flow rate of ~4 mL/min. The optimum conditions for CO_2 activation temperature and gas flow were achieved by analyzing the balance between improvement in surface properties and material loss. The synthesized sample was collected after it was cooled down to room temperature under argon gas purging. The working electrodes for electrochemical evaluations were prepared using slurry of CA powder with 10 wt% polyvinyl alcohol (PVA) solution in water as binder in weight ratio of 1:3. Glutaric acid as esterifying agent was added to the mixture for cross-linking of PVA to get water-insoluble film [23].The slurry was spread uniformly on graphite sheet of the size 20 × 20 cm resulting in total active material loading of 6 g for each electrode. The coating was further cured in inert atmosphere at 130˚C to obtain CA electrode.

2.2. Characterization for morphology, surface area, and specific capacitance

Scanning electron microscopy (SEM) of CA samples prepared with different R/C molar ratio was carried out using Zigma (Carl Zeiss) system to study their surface morphology. The surface area and PSD

of CA samples with different catalyzing and activation conditions were characterized by analysis of nitrogen adsorption–desorption isotherms measured by ASAP-2020 analyzer (Micromeritics). The samples were degassed at 350°C for 10 h prior to the adsorption measurements. BET method was used for total surface area measurements, and *t*-plot method was used for estimating mesopore surface area. PSDs were obtained by the BJH method from desorption branch of the isotherms. Total pore volume was calculated from the adsorbed volume of nitrogen at $P/P_0 = 0.99$ (saturation pressure). In order to compare the electro-sorption behavior of CA samples cyclic voltammetry (CV) was performed. This characterization is a preliminary method to investigate the electro-sorption behavior of a material. Measurements were performed with AUTOLAB PGSTAT302 potentiostat in a conventional three electrode cell. The working electrode of size 1.5 cm^2 was formed using CA material under test as described above. Platinum electrode was used as counter electrode and Ag/AgCl electrode was used as a reference electrode. Measurements were performed in the potential range of −0.5 to + 0.5 volts in 1 M NaCl electrolyte in a manner similar to the method used by Wang et al. [5] and Liu et. al. [8]. The samples were subjected to scan rates of 2, 5, 10, and 20 mV/s. The specific capacitance (*C*) of each electrode was evaluated from CV curves using the relationship $C = I/Sm$, where I (mA) is the average current in the applied potential window, S is applied scan rate in mV/s, and m is mass of active material(mg).

2.3. CDI experiments

Electrosorptive removal of NaCl was measured in batch mode using a continuous recycling system incorporating CDI unit cell, peristaltic pump, a power supply, and a conductivity monitor (Fig. 1). Two electrodes of size 20 × 20 cm were mounted with ~2 mm separation having ~70 mL capacity in CDI unit cell. In a typical experiment 240 mL NaCl solution having an initial concentration of 500 mg/L was employed as feed solution with flow rate 50 mL/min. A direct voltage of 1.2 V was applied between the two working electrodes. The variation of solution conductivity was monitored by conductivity meter (WTW, Cond 330i). The corresponding concentration could be obtained with a calibration curve made prior to the experiments. Salt-adsorption capacity (Q) defined as salt adsorbed per gram of electrode material was calculated according to the following equation:

$$Q(\text{mg/g}) = (C_i - C_f)V/M \quad (1)$$

where C_i and C_f represent the initial and final concentration in mg/L, V is the volume of the solution in L, and M is the mass of active material in gram [24].

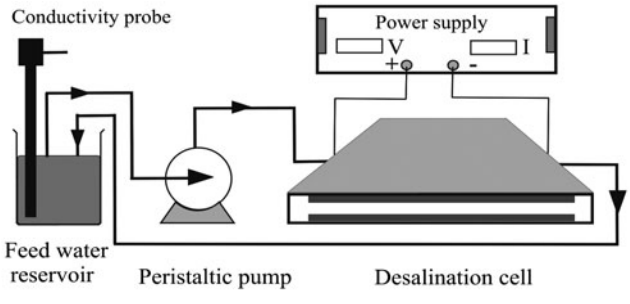

Fig. 1. Schematic diagram of test cell for CDI experiment.

3. Results and discussion

3.1. Morphological examination

Fig. 2(a)–(c) SEM images showing morphologies of the CA obtained at different R/C molar ratios of 100, 300, and 500 (samples RFC-100, RFC-300 and RFC-500). It is seen that CAs are composed of clusters of interconnected carbon nanoparticles of different diameters resulted in continuous porous network. CA derived for RFC-100 (Fig. 2(a)) shows that it has highly dense structure having small particle clusters with mainly micropores. For RFC-300 the image shows network of uniform particles of size ~10 nm with well-developed open and small mesopores. As R/C increases to 500, the particle size and pores size grows further and bigger mesopores dominates.

3.2. Surface area analysis of CAs

Surface area analysis of the synthesized CA by N_2 adsorption showed a strong influence of the R/C molar ratio in textural characteristic (Fig. 3(a) and (b)). It can be seen that the hysteresis in the gas adsorbed vs. relative pressure shifts towards higher pressures with increase in R/C molar ratio indicating the formation of bigger mesopores during gelation process. Sample RFC-100 exhibits a type I isotherm according to Brunnauer–Deming–Deming–Teller classification indicating the predominance of microporosity. The small hysteresis loop in the desorption branch at P/P_0 0.4 shows contribution of mesopores of small size for RFC-200. As R/C molar ratio was increased to 300 the CA displayed a much more developed mesopores structure showing type IV isotherm, with prominent

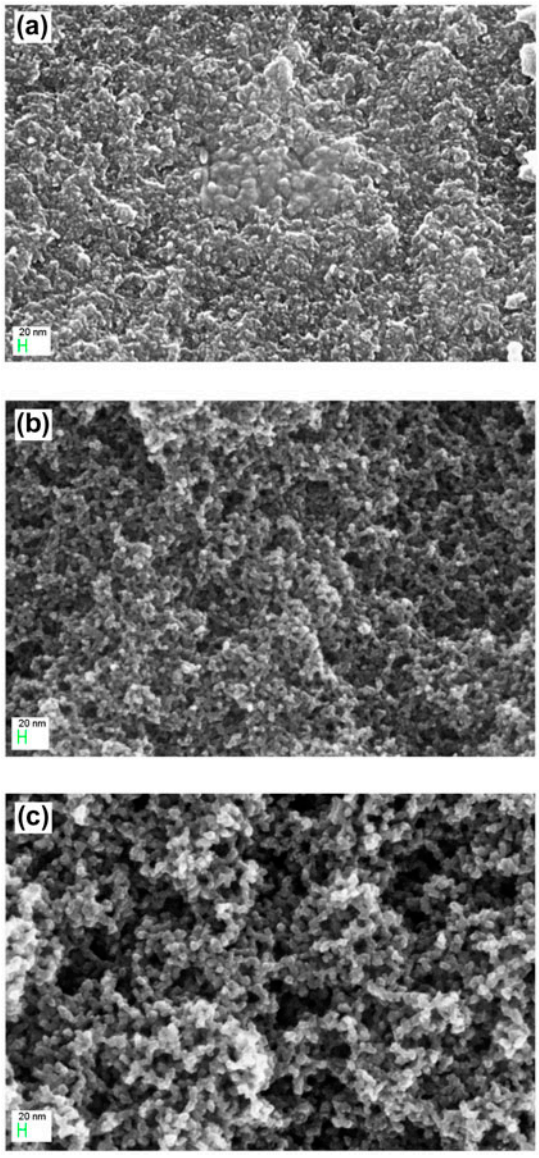

Fig. 2. Scanning electron micrographs of (a) RFC-100 (b) RFC-300 (c) RFC-500.

hysteresis loops at relatively high pressures of P/P_0 0.6. For R/C of 400 and 500 the hysteresis shifts to P/P_0 of 0.7 and 0.8, respectively, indicating presence of bigger mesopores. Fig. 3(b) shows PSD of samples RFC-100, RFC-200, RFC-300, RFC-400, and RFC500 showing that mean pore size increases with the R/C molar ratio. The RFC-100 sample shows the PSD with major contribution of pores below 4 nm diameter. A BJH desorption average pore size lies at 3.6, 8.6, 12.2, and 20.8 for RFC-200, RFC-300, RFC-400, and RFC-500, respectively. These results are in good agreement with the previous works reported in the literature on the porosity development of CA prepared with different R/C molar ratio [21].

Surface area properties of CA prepared with different R/C molar ratio are tabulated in Table 1. Pore volume and average diameter increase with the increase in R/C molar ratio. This behavior is expected because with increasing R/C molar ratio, the catalyst content reduces, resulting in formation of bigger pores. For R/C from 100 to 300, it is observed that both surface areas and pore volume are increasing. But for RFC-400 and RFC-500, although pore volume is increasing because of the presence of bigger mesopores >10 nm, the surface area is decreasing. It emerges that among the prepared samples, RFC-300 has sufficiently high pore size to overcome diffusional limitation of ions as well as highest total surface area and mesopore surface area (698, 289 m^2/g).

3.3. Effect of CO_2 activation on the porous structure of CA

Among the samples prepared with different R/C molar ratio, RFC-300 has highest total as well as mesopore surface area and the average pore size is ~8.6 nm which is sufficient for fast ion kinetics inside pores. The surface area properties of this sample were improved by CO_2 activation to achieve better salt-adsorption capacity. CO_2 activation was carried

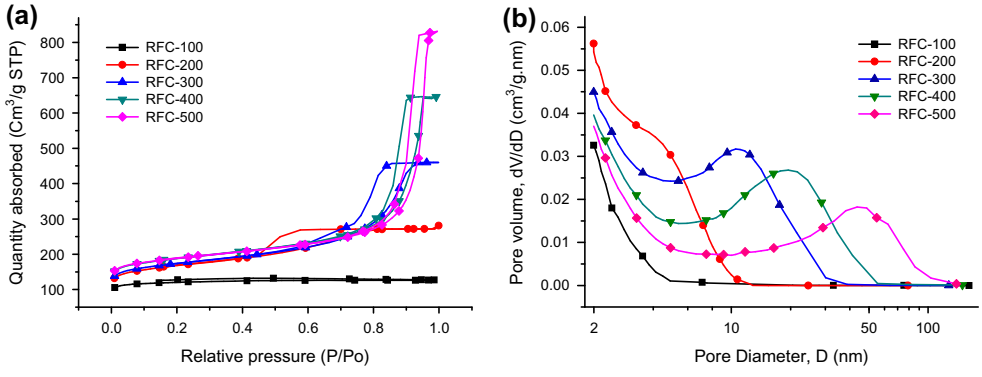

Fig. 3. (a) Adsorption isotherms at 77 K and (b) PSD of CA with different R/C molar ratios.

Table 1
Surface characteristics of CA samples prepared with different R/C molar ratio

Sample	S_{BET} (m^2/g)	S_{Meso} (m^2/g)	Pore V_{total} (cm^3/g)	Pore D_{av} (nm)
RFC-100	490	52	0.21	2.4
RFC-200	604	210	0.39	3.6
RFC-300	698	289	0.79	8.6
RFC-400	628	224	1.13	12.2
RFC-500	601	178	1.33	20.8

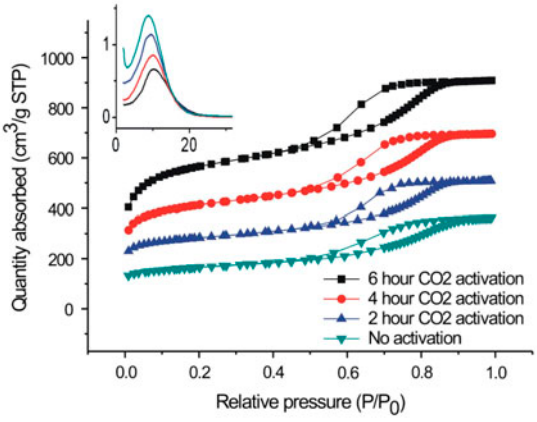

Fig. 4. CO_2 activation isotherms with inset showing dV/dlog(D) vs. pore diameter D (nm) for RFC-300 with different activation duration.

out at 950°C with varying activation time and corresponding N_2 isotherms are shown in Fig. 4. The surface properties of CO_2 activated CA are summarized in Table 2. Activation causes improvement in surface area accompanied by material loss due to burn-off. The isotherms show a steep increase in the amount of gas adsorbed at low P/P_0 indicating that large quantity of micropores has been introduced after activation. This might be due to the creation of new micropores by oxidation of certain structural components and opening of previously inaccessible pores. The isotherms are shifted upwards and area under hysteresis is also marginally increased with activation time which indicates that there is an increase in the area of both micro and mesopores. For all the isotherms shown in Fig. 4 hysteresis loops are located almost over the same P/P_0 range indicating that activation process does not affect the size of pores and PSD significantly. The surface area was found to increase from 698 to 2057 m^2/g (mesopore surface area from 289 to 644 m^2/g) after 6 h activation. It can be observed that although the average diameters of pores with different activation times are slightly decreasing, there is a significant increase in pore volume. For higher activation duration, percentage increase in surface area is overtaken by material burn-off hence 6 h activation was the optimum. The changes observed in the porous structure of the studied samples are reflected in difference in their electrochemical performance.

3.4. Specific capacitance measurements

The CV profiles of the electrodes prepared with CA synthesized at different R/C molar ratio measured at a scan rate of 10 mV/s were displayed in Fig. 5. The closed area of CV curve is an indicator of capacitance of the material. Profiles show quasi-rectangular symmetric and reversible shape in the voltage range −0.5 to 0.5 V. There are no additional oxidation/reduction peaks observed in the chosen potential range, suggesting the ideal capacitive behavior. It is observed that as we proceed from RFC-100 to RFC-500, the CV curve approaches towards rectangular shape which is due to fast ion kinetics for bigger pores. For RFC-500 although the shape is nearly rectangular but the capacitance is lower as bigger mesopores diminishes total surface area. The maximum specific capacitance of 61 F/g was obtained

Table 2
Surface properties of RFC-300 with CO_2 activation

Activation duration	S_{BET} (m^2/g)	S_{Meso} (m^2/g)	Pore V_{total} (cm^3/g)	Pore D_{av} (nm)	% Burn-off
No activation	698	289	0.79	8.6	6
2 h	1,142	424	0.91	7.9	15
4 h	1,647	547	1.01	7.0	25
6 h	2057	644	1.72	6.6	40
8 h	2,298	705	1.89	6.3	70

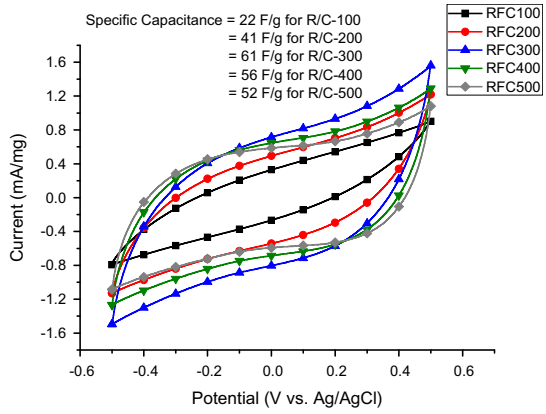

Fig. 5. CV curves for samples with different R/C molar ratio at 10 mV/s scan rate.

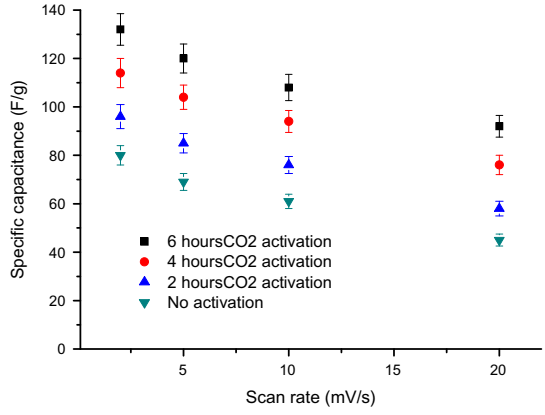

Fig. 6. Specific capacitance of RFC-300 with varying CO_2 activation time at different scan rates.

for RFC-300 which has highest total as well as mesopore surface area among the selected samples.

RFC-300 was further activated by CO_2 for different hours and its specific capacitance was evaluated. The calculated specific capacitance values obtained at different scan rates from CV curve are plotted in Fig. 6. It is observed that significant improvement in capacitance was obtained with increasing activation duration as increase in activation leads to improvement in surface area and pore volume of CA. The decrease in capacitance for all the samples with scan rate is not very pronounced as for selected sample PSD is sufficiently high to overcome diffusional limitation. Specific capacitance values for untreated RFC-300 at scan rate of 2, 5, 10, and 20 mV/s were 80, 69, 61, and 45 F/g and after CO_2 activation for 6 h, the values significantly improved to 132, 120, 108, and 92 F/g, respectively. The values are higher than those reported for the ambient dried CA [22]. The higher capacitance values imply higher efficiency in removing salt ions by electrosorption desired for better desalination performance.

3.5. CDI performance

The CDI behaviors of electrodes prepared using sample RFC-300 (untreated and activated for 6 h) were evaluated with a self-made batch mode desalination apparatus. The change in concentration of solution was recorded during adsorption and desorption cycles and resultant profiles exhibited in Fig. 7. During desorption cycle at 0 V, concentration builds up to original value indicates nearly complete regeneration. In adsorption cycle, the concentration decreased from 500 to 292 ppm for untreated CA and to 88 ppm for CO_2 activated CA. The calculated salt-adsorption capacity according to equation 1 is 4.1 and 8.4 mg/g, respectively. The salt-adsorption capacity obtained for the CO_2 activated sample is significantly higher than the values reported earlier [24]. The synergetic effect of higher specific surface area and appropriate PSD is believed to be responsible for high electrosorption capacity. Fig. 7(b)

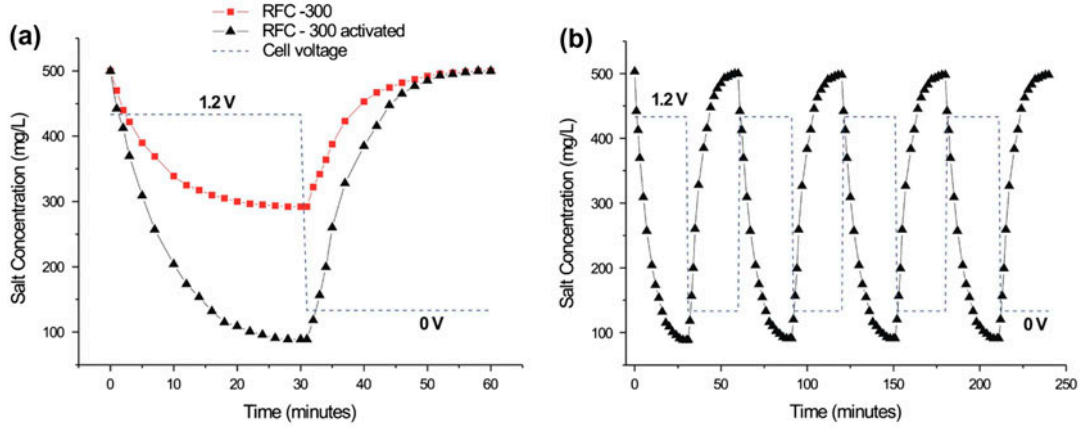

Fig. 7. (a) Concentration change in adsorption and desorption cycle (b) Sample performance in multiple cycles.

shows performance stability of sample in multiple cycles.

4. Conclusions

CAs were synthesized through polycondensation of resorcinol with formaldehyde by ambient drying method. By varying the catalyzing conditions of the precursor solution, the surface morphology and pore distribution could be tailored and CA with mesopores with average pore diameter of 9 nm was obtained. The surface textural properties of the CA generated were remarkably increased by CO_2 activation at 950°C. The electrosorption behavior of prepared material was investigated by CV which displayed stable and superior specific capacitance after activation. The batch mode CDI experiments reveal that the material after activation has salt-adsorption capacity of 8.4 mg/g of active material. The enhanced electrosorption behavior of the activated CA electrode can be ascribed to well-controlled PSD with improved surface area.

Acknowledgment

We would like to thank Shri Gopal Mohod for his help at various stages to carry out desalination experiments.

References

[1] T.J. Welgemoed, C.F. Schutte, Capacitive deionization technology™: An alternative desalination solution, Desalination 183 (2005) 327–340.
[2] Y. Oren, Capacitive deionization (CDI) for desalination and water treatment—Past, present and future (a review), Desalination 228 (2008) 10–29.
[3] L. Zou, G. Morris, D. Qi, Using activated carbon electrode in electrosorptive deionisation of brackish water, Desalination 225 (2008) 329–340.
[4] H. Li, Y. Gao, L. Pan, Y. Zhang, Y. Chen, Z. Sun, Electrosorptive desalination by carbon nanotubes and nanofibres electrodes and ion- exchange membranes, Water Res. 42 (2008) 4923–4928.
[5] Z. Wang, B. Dou, L. Zheng, G. Zhang, Z. Liu, Z. Hao, Effective desalination by capacitive deionization with functional graphene nanocomposite as novel electrode material, Desalination 299 (2012) 96–102.
[6] L. Li, L. Zou, H. Song, G. Morris, Ordered mesoporous carbons synthesized by a modified sol–gel process for electrosorptive removal of sodium chloride, Carbon 47 (2009) 775–781.
[7] P. Xu, J.E. Drewes, D. Heil, G. Wang, Treatment of brackish produced water using carbon aerogel-based capacitive deionization technology, Water Res. 42 (2008) 2605–2617.
[8] Y. Liu, W. Ma, Z. Cheng, J. Xu, R. Wang, X. Gang, Preparing CNTs/Ca-Selective zeolite composite electrode to remove calcium ions by capacitive deionization, Desalination 326 (2013) 109–114.
[9] H.B. Li, L.K. Pan, T. Lu, Y.K. Zhan, C.Y. Nie, Z. Sun, A comparative study on electrosorptive behavior of carbon nanotubes and graphene for capacitive deionization, J. Electroanal. Chem. 653 (2011) 40–44.
[10] Y.J. Kim, J.H. Choi, Enhanced desalination efficiency in capacitive deionization with an ion-selective membrane, Sep. Purif. Technol. 71 (2010) 70–75.
[11] X.Z. Wang, M.G. Li, Y.W. Chen, R.M. Cheng, S.M. Huang, L.K. Pan, Z. Sun, Electrosorption of ions from aqueous solutions with carbon nanotubes and nanofibers composite film electrodes, Appl. Phys. Lett. 89 (2006) 053127.
[12] J.C. Farmer, D.V. Fix, G.V. Mack, R.W. Pekala, J.F. Poco, Capacitive deionization of NH_4ClO_4 solutions with carbon aerogel electrodes, J. Appl. Electrochem. 26 (1996) 1007–1018.
[13] F. Duan, Y. Li, H. Cao, Y. Xie, Y. Zhang, Capacitive deionization by ordered mesoporous carbon: Electrosorption isotherm, kinetics, and the effect of modification, Desalin. Water Treat. (2013) 1–8.
[14] D.K. Kohli, R. Singh, M.K. Singh, A. Singh, R.K. Khardekar, P. Ram Sankar, P. Tiwari, P.K. Gupta, Study of carbon aerogel-activated carbon composite electrodes for capacitive deionization application, Desalin. Water Treat. 49 (2012) 130–135.
[15] S. Nadakatti, M. Tendulkar, M. Kadam, Use of mesoporous conductive carbon black to enhance performance of activated carbon electrodes in capacitive deionization technology, Desalination 268 (2011) 182–188.
[16] R.W. Pekala, Organic aerogels from the polycondensation of resorcinol with formaldehyde, J. Mater. Sci. 24 (1989) 3221–3227.
[17] D. Wu, R. Fu, S. Zhang, M.S. Dresselhaus, G. Dresselhaus, Preparation of low-density carbon aerogels by ambient pressure drying, Carbon 42 (2004) 2033–2039.
[18] D. Wu, R. Fu, M.S. Dresselhaus, G. Dresselhaus, Fabrication and nano-structure control of carbon aerogels via a microemulsion-templated sol–gel polymerization method, Carbon 44 (2006) 675–681.
[19] T. Yamamoto, T. Nishimura, T. Suzuki, H. Tamon, Control of mesoporosity of carbon gels prepared by sol-gel polycondensation and freeze drying, J. Non-Cryst. Solids 288 (2001) 56–55.
[20] S. Guo, J. Peng, W. Li, K. Yang, L. Zhang, S. Zhang, H. Xia, Effects of CO2 activation on porous structures of coconut shell-based activated carbons, Appl. Surf. Sci. 255 (2009) 8443–8449.
[21] H. Tamon, H. Ishizaka, T. Araki, M. Okazaki, Control of mesoporous structure of organic and carbon aerogels, Carbon 36 (1998) 1257–1262.
[22] Y.J. Lee, J.C. Jung, J. Yi, S.H. Baeck, J.R. Yoon, I.K. Song, Preparation of carbon aerogel in ambient conditions for electrical double-layer capacitor, Curr. Appl. Phys. 10 (2010) 682–686.
[23] B.H. Park, Y.J. Kim, J.S. Park, J. Choi, Capacitive deionization using a carbon electrode prepared with water-soluble poly(vinyl alcohol) binder, J. Ind. Eng. Chem. 17 (2011) 717–722.
[24] G. Wang, C. Pan, L. Wang, Q. Dong, C. Yu, Z. Zhao, J. Qiu, Activated carbon nanofiber webs made by electrospinning for capacitive deionization, Electrochim. Acta 69 (2012) 65–70.